Applied Catalysis B: Environmental 84 (2008) 277–288

Contents lists available at ScienceDirect

Applied Catalysis B: Environmental

journal homepage: www.elsevier.com/locate/apcatb

Nitrous oxide decomposition over transition metal exchanged ZSM-5 zeolites prepared by the solid-state ion-exchange method

Bahaa M. Abu-Zied [a,1,*], Wilhelm Schwieger [b], André Unger [b,2]

[a] Chemistry Department, Faculty of Science, Assiut University, 71516 Assiut, Egypt
[b] Institut Für Chemische Reaktionstechnik, Friedrich-Alexander-Universität Erlangen-Nürnberg, Egerlandstraße 3, 91058 Erlangen, Germany

ARTICLE INFO

Article history:
Received 31 December 2007
Received in revised form 28 March 2008
Accepted 5 April 2008
Available online 11 April 2008

Keywords:
Nitrous oxide
Solid-state ion-exchange
Co-ZSM-5
Cu-ZSM-5
Fe-ZSM-5

ABSTRACT

This paper studied nitrous oxide decomposition over a series of transition metal exchanged ZSM-5 zeolites prepared by solid-state ion-exchange method. Crystallographic structure of the catalysts has been investigated with the aid of XRD analysis. The texture of the prepared catalysts was investigated using nitrogen sorption. FTIR measurements applying pyridine as a probe molecule have been carried out in order to investigate the nature of the acid sites of the different catalysts. In situ electrical conductivity measurements were carried out in order to relate the activity of this series of catalysts to their electrical conductivity variation in the presence of N_2O. The obtained results revealed that the N_2O decomposition activity is related to the relative conductivity decrease upon the admission of N_2O over metal exchanged ZSM-5 zeolites. Further studies have been performed over Co-, Cu- and Fe-ZSM-5 catalysts since they showed the highest activity patterns among all the tested catalysts. Such studies included the effect of changing Si/Al ratio, the exchange level, the calcination temperature and the milling time.

1. Introduction

The study of the catalytic decomposition of nitrous oxide has gained more attention because N_2O was cited according to the Kyoto Protocol as a non-CO_2 greenhouse gas. Nitrous oxide is also known to participate in the destruction of the stratospheric ozone layer [1–4]. In this context, it was reported that a doubling in the atmospheric laughing gas concentration could result in 12% decrease in the total stratospheric ozone [4]. In the recent years an increased number of articles was published aiming to suggest routes for the reduction of nitrous oxide emission (see for example refs. [3–57]). The suggested solutions include, (i) utilization of N_2O in the selective oxidation of methane to methanol [5,6] and benzene to phenol [6–18], (ii) direct catalytic decomposition of N_2O into its elements [3,19–41], and (iii) selective catalytic reduction (SCR) of N_2O with ammonia [41–43], carbon monoxide [44–49] and hydrocarbons [4,50–57]. Among the catalysts tested for N_2O conversion metal exchanged ZSM-5 zeolites exhibited promising activity features. This is not only true for the direct decomposition [3,19–26,35–41] and the SCR of N_2O [4,41–45,50–57], but also for the SCR of NO [58–60]. Moreover, enhancement effect of NO for the direct N_2O decomposition was reported over Fe-ZSM-5 catalysts [61,62].

Different preparation methods have been utilized for the preparation of transition metal exchange ZSM-5 catalysts. These include conventional ion exchange in aqueous solution, solid-state ion-exchange (SSIE), sublimation or chemical vapour deposition and the ex-framework method, i.e. M-ZSM-5 which contains extra-framework metal species prepared by calcinations and steam treatment of M-ZSM-5. In this context, it was reported that Fe-ZSM-5 prepared by the SSIE method is more active towards direct N_2O decomposition than that obtained via aqueous ion exchange [20,41]. The same authors [20] also showed that ex-frame Fe-ZSM-5 is more active than Fe-ZSM-5 prepared by the SSIE methods towards the same reaction. Meanwhile, approximately similar activity features were reported for Fe-ZSM-5 prepared by the SSIE and the chemical vapour deposition [63]. Kögel et al. [50] revealed that Fe-ZSM-5 prepared via the SSIE method has a high activity in N_2O reduction with propane in the presence of NO. The same catalyst exhibited also high activity during NO reduction with isobutane [64]. SSIE method was applied also for the preparation of active Co-ZSM-5 in the ammoxidation of ethane to acetonitrile [65].

In the preparation of transition metal exchanged ZSM-5 catalysts H- or NH_4-forms of the zeolite powder are mixed with

* Corresponding author. Tel.: +20 12 2942778; fax: +20 88 2342708.
E-mail addresses: babuzied@aun.edu.eg (B.M. Abu-Zied), schwieger@rzmail.uni-erlangen.de (W. Schwieger), andre.unger@parrinst.de (A. Unger).
[1] On leave from Assiut University.
[2] Present address: Parr Instrument (Deutschland) GmbH, Zeilweg 15, 60439 Frankfurt am Main, Germany.

0926-3373/$ – see front matter © 2008 Elsevier B.V. All rights reserved.
doi:10.1016/j.apcatb.2008.04.004

a metal salt (usually chloride). Uniform mixtures are obtained by using ball milling [65]. However, mixing with agate mortar was also reported [66]. The obtained mixture is then heated in air, inert atmosphere or vacuum. During the thermal treatment, the solid-state interaction occurs which is accompanied by evolution of HCl or NH_4Cl gases, respectively. Generally, solid-state ion-exchange method has the following advantages: (i) it allows the control of the metal loading, (ii) it allows the exchange of multivalent cations into zeolite site which is normally very difficult because of the large size of the hydrated metal complex [65], (iii) it is reproducible even in the presence of air atmosphere, (iv) it can create some active sites that are different from those obtained by aqueous exchange [65], and (v) it allows the control of the crystallite size. Such properties facilitate the solid-state ion-exchange method to be applied in the large-scale manufacture of metal exchanged zeolite catalysts. The present investigation was undertaken to shed some light on the activity of a series of transition metal exchanged ZSM-5 catalysts, prepared via the SSIE method, towards direct N_2O decomposition. Further experiments were carried out on the most active catalysts, namely Co-, Cu- and Fe-ZSM-5 catalysts. This includes the influence of Si/Al ratio, exchange level, calcination temperature and milling time.

2. Experimental

2.1. Catalysts preparation

The zeolite ZSM-5 materials with different Si/Al ratios (25, 40, 50, 100, 150, and 200) were synthesized in a 2 L stirring autoclave through hydrothermal crystallization of a reaction mixture starting from sodium aluminate as the Al_2O_3 source, colloidal silicic acid as the SiO_2 source, and tetrapropylammonium-bromide (TPABr) as the template according to the procedure reported recently [18]. The chemical composition determined by ICP yields iron content less than 0.01 wt.% for all samples. The ammonium form of the Na-ZSM-5 zeolites was prepared by the conventional ion exchange with ammonium nitrate solution (2 M) at 95 °C under stirring. The working procedure was done for three times, 15 min stirring at 95 °C for the first two exchanges and 3 h stirring for the last one. The obtained NH_4-ZSM-5 zeolites were, then, dried at 110 °C for 16 h.

Transition metal-exchanged ZSM-5 zeolites were obtained by solid-state ion-exchange (SSIE) of its ammonium form as reported previously [50,62]. Briefly, 5 g of the parent zeolite was mechanically mixed with the transition metal chlorides or nitrates in case of silver and cerium ions (adjusted to achieve 100% exchange level taking into account the metal oxidation state, for example in case of silver; Ag/Al = 1.0, for copper; Cu/Al = 0.5) for 1 h in a ball mill (type Fritsch, which contains 5 balls). Subsequently, the mixture was heated to 550 °C within 3 h in chamber furnace and kept at this temperature for 6 h under static air conditions. During this thermal treatment the ion exchange between the NH_4^+ ions of the zeolite and the metal cations of the salt takes place. Afterwards the product was cooled down to ambient temperature, washed intensively with de-ionized water to remove the adsorbed chloride ions and then dried at 110 °C for 16 h. Finally, the obtained catalysts were pressed to tablets, crushed and sieved to obtain fractions of 630–800 μm. The obtained samples were denoted as M-ZSM-5, where M denotes the metal cation used.

2.2. Characterization of the catalysts

Chemical composition of the different catalysts was determined by using inductively coupled plasma atomic emission spectroscopy (ICPAES) using a PerkinElmer Plasma 400 emission spectrometer. The samples were dissolved in a mixture of concentrated HCl, HNO_3, and HF. Powder X-ray diffractograms were obtained in the 2θ range 5–80° with the aid of Philips X-Pert-Pro using the Ni-filtered CuKα radiation. Adsorption–desorption isotherms of nitrogen (at −196 °C) were conducted with the aid of ASAP 2010, Micromeritics gas sorption apparatus. The catalysts were evacuated at 250 °C for 4 h before the nitrogen adsorption measurements. Micropore-surface area as well as micropore-volume of some catalysts was evaluated using Dubinin–Astakhov method. Pyridine adsorption was used to investigate the nature of the acid sites. Approximately 10 mg were pressed into thin wafers using a 13 mm diameter die and applying 10 ton pressure. The obtained wafers were mounted on a quartz holder and installed in a quartz glass vacuum chamber. Prior to pyridine adsorption, the wafers were activated by heating them under vacuum at 350 °C for 2 h. Following activation the samples were allowed to cool to 200 °C and pyridine vapour was admitted for 45 min. A second pyridine step was done by admitting pyridine vapour for 30 min at 160 °C. This is to be sure that enough pyridine is adsorbed on the zeolites. The wafers were, then, cooled to 140 °C and evacuated for 2 h. Finally, the wafers were allowed to cool down to room temperature and, then, the glass chamber was transferred to FTIR spectrophotometer. FTIR spectra were recorded using PerkinElmer VX170 spectrophotometer.

2.3. Activity and in situ electrical conductivity measurements

The catalytic measurements were carried out in an electrically heated quartz tube reactor. The temperature in the reactor was measured using a thermocouple on the catalyst bed. Prior to each experiment 500 mg catalyst were treated in He at 550 °C for 1 h and then cooled to the desired temperature. The concentration of reactant gas, 500 ppm N_2O, was added with the aid of Bronkhorst thermal mass flow controllers using He as a balance gas, the volumetric flow rate was 125 $cm^3\,min^{-1}$ (NTP). The gases used were all of >99% purity and He was >99.999% purity, and they were used without further purification. The exit concentrations were monitored by means of non-dispersive infrared analyzer for the N_2O (Hartmann and Braun, Uras 10E). The steady state was reached after 30 min to 1 h for the different catalysts tested. In situ electrical conductivity measurements were carried out using a conductivity cell similar to that described by Chapman et al. [67]. The resistance measurements were carried out using a Keithley 610 C solid-state electrometer. In each run 500 mg of the catalyst were placed between two electrodes (1.0 cm diameter) and pressed by the upper electrode in order to ensure a good contact between the particles. The cell was heated to 500 °C and the electrical conductivity was monitored till a steady value was reached (σ_0). Then, 500 ppm N_2O in nitrogen was introduced to the cell with the aid of Aalborg thermal mass flow controllers, in a flow rate of 200 $cm^3\,min^{-1}$ (NTP) and the values of the electrical conductivity were recorded with time (σ).

3. Results and discussion

3.1. Chemical composition and X-ray diffraction

Table 1 shows the chemical composition of the H-ZSM-5 as well as the different transition metal containing ZSM-5 zeolites. The Si/Al ratio in all the solids agreed well with the nominal value and, as expected, did not experience significant changes upon SSIE treatment. The transition metals content; approximately similar values to the nominal ones were observed for the most of the catalysts. This in turn confirms that the washing step in the working procedure applied did not lead to a significant metal loss.

Table 1
XRD crystallinity and chemical analyses of H-form and the different transition metal exchanged ZSM-5 zeolites (Si/Al = 25)

Catalyst	Metal salt	Adjusted M/Al ratio	ICP determined elements			M/Al	XRD Crystallinity [%][b]
			M [wt.%]	Si [wt.%]	Al [wt.%]		
H-ZSM-5	–	–	–	39.12	1.49	–	100
Cd-ZSM-5	$CdCl_2 \cdot H_2O$	0.5	2.71	37.33	1.41	0.46	81
Ce-ZSM-5	$Ce(NO_3)_3 \cdot 6H_2O$	0.33	n.d.	37.15	1.44	n.d.	73
Co-ZSM-5	$CoCl_2$[a]	0.5	1.56	36.39	1.42	0.50	91
Cu-ZSM-5	$CuCl_2 \cdot 2H_2O$	0.5	1.62	38.46	1.47	0.47	98
Fe-ZSM-5	$FeCl_2 \cdot 4H_2O$	0.5	1.71	43.77	1.66	0.50	83
La-ZSM-5	$LaCl_3 \cdot 7H_2O$	0.33	n.d.	39.49	1.52	n.d.	94
Mn-ZSM-5	$MnCl_2 \cdot 4H_2O$	0.5	1.36	36.49	1.36	0.49	84
Ni-ZSM-5	$NiCl_2 \cdot 6H_2O$	0.5	1.58	37.09	1.43	0.51	91
Pd-ZSM-5	$PdCl_2$[a]	0.5	3.20	39.46	1.53	0.53	79
Ag-ZSM-5	$AgNO_3$[a]	1.0	6.21	38.50	1.49	1.04	95
Y-ZSM-5	$YCl_3 \cdot 7H_2O$	0.33	n.d.	37.68	1.48	n.d.	81
Zn-ZSM-5	$ZnCl_2$	0.5	1.74	38.29	1.43	0.50	91

n.d.: not determined.
[a] Anhydrous state.
[b] Calculated according to ref. [18].

In agreement, it was shown earlier [50] that no iron is lost during the SSIE method and calcinations during the preparation of Fe-ZSM-5 catalysts.

In order to check the crystallinity of the different M-ZSM-5 catalysts (Si/Al = 25) after the solid-state ion-exchange and the possible formation of metal oxides, XRD analysis was carried out. The powder diffractograms of the various catalysts (Fig. 1a) were similar to that obtained for H-ZSM-5 in this and other studies [10,68–70], confirming that the utilized procedure did not affect the structure of the zeolite. Moreover, the intensities of the MFI peaks in the M-ZSM-5 catalysts are similar to those of the parent H-ZSM-5. Meanwhile, the obtained diffractograms (Fig. 1b) reveal the presence of a minor amount of PdO, Ag_2O and NiO in their corresponding zeolites (JCPDS cards no. 85–0713, 76–1393 and 78–0643, respectively). In this context, Koyano et al. [71] have detected PdO for their Pd/H-ZSM-5 and Pd/Na-ZSM-5 catalysts prepared by ion exchange from solution. Hence, it seems that the formation of PdO cannot be avoided by using the ion exchange from solution or the SSIE method. No indications of the formation of cobalt, copper and iron or other metals oxides were observed in their corresponding XRD patterns. Consistent with this Fe_2O_3 [72] and CuO [73] were detected in their ZSM-5-containing zeolites when the transition metal content exceeded 5%. Accordingly, one may conclude that these metal oxides aggregates, larger than 5 nm particle size, are not present in the various M-ZSM-5 catalysts (other than PdO, Ag_2O and NiO), since XRD is a bulk sensitive technique that requires crystallites of minimum dimensions near 5 nm [74,75].

3.2. Acidity

The nature of the acid sites was investigated by FTIR analysis. The infrared spectra, in the spectral region 1580–1400 cm^{-1} of adsorbed pyridine on the different M-ZSM-5 catalysts are shown in Fig. 2. All the catalysts show typical bands of adsorbed pyridine at around 1546, 1490 and 1450 cm^{-1}. The bands located at around 1546 cm^{-1} are due to pyridinium ion (PyH^+) reflecting thus its interaction with Brønsted sites. The bands at 1450 cm^{-1} are characteristic for coordinatively bonded pyridine on electron acceptor site (Lewis center). The bands at about 1490 cm^{-1} contain contributions of the two types of acidity [7,76–79]. Pophal et al. [79] examined the acidity of Na-ZSM-5 through pyridine adsorption. Their results revealed the absence of peaks due to adsorbed pyridine on both Lewis and Brønsted sites. Meanwhile, only

Table 2
Acidity and texture characteristics of different transition metal ZSM-5 catalysts prepared by the SSIE method

Catalyst	Adsorbed pyridine area[a]				Exchange Level [%][e]	Micropore Surface area [$m^2\ g^{-1}$]	Micropore Volume [$cm^3\ g^{-1}$]
	Lpy[b]	Bpy[c]	Tpy[d]	Bpy/Lpy			
H-ZSM-5	1.604	6.787	4.685	4.321	–	438	0.177
Cd-ZSM-5	2.205	1.414	1.707	0.641	79	316	0.117
Ce-ZSM-5	2.465	2.505	0.735	1.016	63	n.m.	n.m.
Co-ZSM-5	1.828	2.020	2.437	1.105	70	324	0.121
Cu-ZSM-5	2.689	1.461	2.210	0.543	78	349	0.128
Fe-ZSM-5	0.355	1.949	1.924	5.490	71	432	0.161
La-ZSM-5	0.685	2.410	2.374	3.518	64	n.m.	n.m.
Mn-ZSM-5	1.223	2.029	2.293	1.659	70	322	0.120
Ni-ZSM-5	2.364	1.696	2.248	0.717	75	341	0.128
Pd-ZSM-5	0.636	2.087	2.312	3.281	69	385	0.145
Ag-ZSM-5	5.635	0.346	1.055	0.061	95	n.m.	n.m.
Y-ZSM-5	0.945	2.411	2.447	2.551	64	n.m.	n.m.
Zn-ZSM-5	3.609	0.713	2.506	0.198	89	331	0.122

n.m.: not measured.
[a] Relative areas per 10 mg samples.
[b] Lpy: pyridine adsorbed on Lewis acid sites (corresponds to the area of the band at 1450 cm^{-1}).
[c] Bpy: pyridine adsorbed on Brønsted acid sites (corresponds to the area of the band at 1546 cm^{-1}).
[d] Tpy: total acidity (corresponds to the area of the band at 1490 cm^{-1}).
[e] The exchange level % = $[(B_{pyH\text{-}form} - B_{pyM\text{-}ZSM\text{-}5})/B_{pyH\text{-}form}] \times 100$.

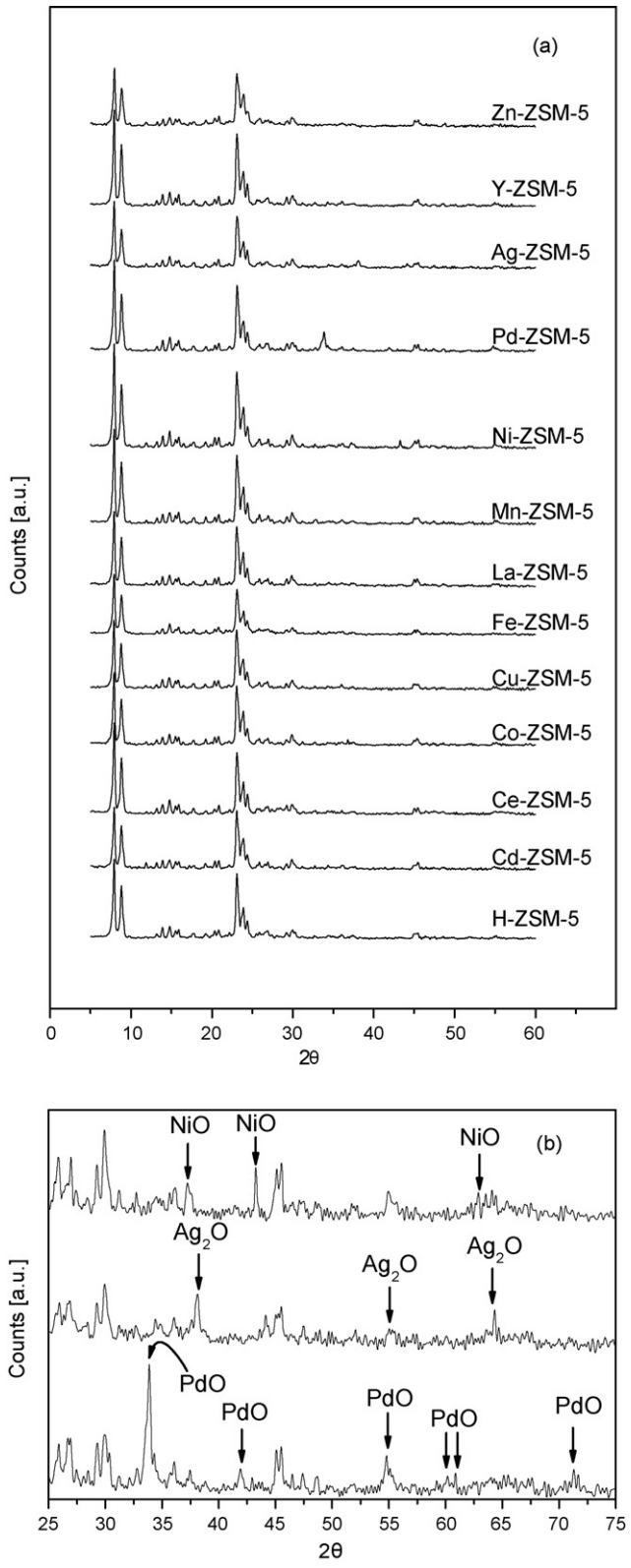

Fig. 1. XRD patterns of the different M-ZSM-5 catalysts.

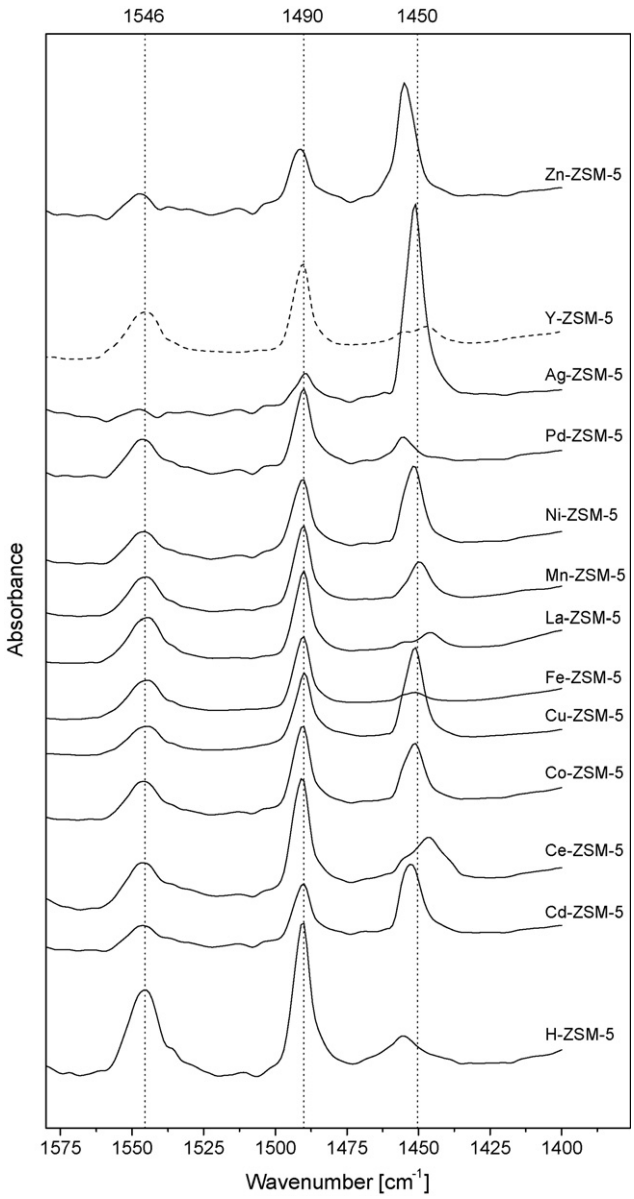

Fig. 2. FTIR spectra of adsorbed pyridine molecules obtained for the different M-ZSM-5 catalysts. The data have been collected at room temperature and the spectra of the pure zeolites have been subtracted.

physisorbed pyridine (Hpy) was detected on the same sample, corresponding to a wavenumber of 1433 cm^{-1}. Under the same conditions, H-ZSM-5 and Fe-ZSM-5 (71% exchange level) showed the absence of such absorption. Inspection of our results (Fig. 2) reveals the absence of any band at around 1433 cm^{-1} for all the tested catalysts. This could be an evidence for the complete removal of sodium ions during the NH_4-form preparation, reflecting the validity of the procedure followed.

Table 2 summarizes the Brønsted and Lewis peak areas together with their ratios for the H-form as well as the different transition metals containing ZSM-5 catalysts. Moreover, in this Table the values of the degree of exchange of Brønsted sites of the different M-ZSM-5 catalysts (calculated from the area of their Brønsted peak areas with respect to that of H-form) are cited. It is evident that Fe-ZSM-5 catalyst shows the lowest Lewis acidity whereas Ag-ZSM-5 exhibits the highest one. On the other hand, Ce- and Ag-containing catalysts show the highest and the lowest Brønsted acidity, respectively. The detection of an increased number of Lewis acid sites, on most of the catalysts, is perhaps not surprising since transition metal cations are electron acceptors. This is in a good agreement with the earlier work carried out on Co- and Fe-ZSM-5 catalysts [75,76]. Comparing the positions of Lewis bands (Fig. 2) shows that, Ce-, Y-, and La-ZSM-5 catalysts exhibit a shift towards

lower wavenumbers. This could indicate the weakening of the bonding to these sites [77]. In addition, Zn-, Cd- and Pd-ZSM-5 catalysts reveal a shift of Lewis bands towards higher wavenumber values, reflecting the strength of the bonding to these sites.

From the M/Al ratios determined by the elemental analysis (Table 1) and the evaluation of the degree of exchange of sites for metal cations (Table 2) one can abstract the following points: (i) even that the same treatment procedure is used, the resulting catalysts exhibit different acidic properties, (ii) due to the fact the still observing a great amount of Brønsted acidity, the process of SSIE does not lead to a sample in which all the active centers are exchanged, (iii) in addition to the metal oxides detected by the XRD analysis (PdO, NiO and Ag_2O), it seems that the rest of the catalysts contain a minor amount of metal oxides containing clusters, (iv) for Ag-ZSM-5 catalyst the obtained pyridine adsorption data suggests a value of 95% exchange level, where the elemental analysis shows Ag/Al close to 1. This seems to be in a contrast with the XRD results where Ag_2O, as an additional phase, was detected. In other words, the detection of Ag_2O phases by the XRD analysis suggests an exchange level lower than 95%. In order to solve such contradiction in situ XRD measurements of this catalyst, from ambient temperature up to 350 °C, were carried out. The obtained results are shown in Fig. 3. It is evident that, the peaks due to Ag_2O decrease with the temperature rise. This, in turn, suggests that silver oxide reacts with the zeolite protons according to:

$$2\text{ZO-H} + Ag_2O \rightarrow 2\text{ZO}^-Ag^+ + H_2O \quad (1)$$

where ZO^- and ZO–H represent the zeolite lattice and acidic protons at Brønsted acid sites, respectively. Hence, it is plausible to suggest that the pre-treatment of this catalyst at 350 °C under vacuum facilitates water vapour evolution. Moreover, the XRD of this sample recorded after cooling (not shown) is quit similar to that recorded at the beginning of the measurements suggesting the reversibility of this process.

3.3. Catalytic activity

3.3.1. Comparison of the metal exchanged ZSM-5 catalysts

Fig. 4 shows the temperature dependence of N_2O conversion over the different transition metal exchanged ZSM-5 as well as the H-ZSM-5 catalysts. In comparison to the parent zeolite, i.e. H-ZSM-5, the examined catalysts can be divided into two groups. The first one (group A), which shows higher activity patterns than that of the parent H-ZSM-5, includes Fe-, Cu-, Co-, Pd-, Ag-, Ce- and La-ZSM-5 (Fig. 4a). On the other hand, the second group (group B) includes Ni-, Y-, Mn-, Zn-, and Cd-ZSM-5 catalysts (Fig. 4b). This series exhibits lower activity values than those of H-ZSM-5.

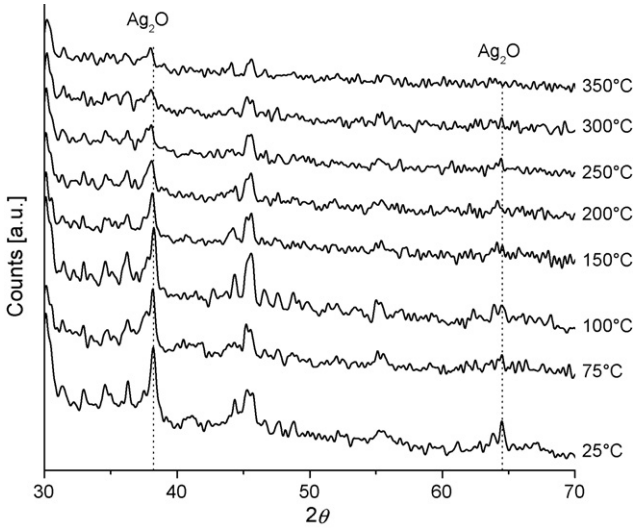

Fig. 3. In situ XRD diffractograms obtained for Ag-ZSM-5 catalyst during heating from ambient till 350 °C.

Regarding the N_2O decomposition on the group A catalysts (Fig. 4a), the onset of the reaction occurs at ca. 250, 275 and 300 °C for Co-, Cu- and Fe-ZSM-5 catalysts, respectively. For the other catalysts in the same series, it is evident that the onset of the reaction starts at higher reaction temperatures (375–450 °C). The N_2O conversion rises very rapidly with temperature on Cu- and Fe-ZSM-5 catalysts, more smoothly on Co-ZSM-5 as well as the rest of the catalysts in this series. The metals in this series can be arranged in the sequence of decreasing activity for the direct N_2O decomposition:

$$\text{Cu} \approx \text{Fe} > \text{Co} \gg \text{Pd} > \text{Ag} \approx \text{Ce} > \text{La}$$

However, in the low temperature region (<350 °C) Co-ZSM-5 catalyst shows higher activity than both copper and iron catalysts. Going to the other series of catalysts (Fig. 4b), the onset of the reaction starts at temperatures as high as 400–475 °C. The N_2O decomposition increases with raising the temperature over all the catalysts in this series whereas the maximum conversion did not exceed 40% at 550 °C. The activity of the metal ion-exchanged zeolite catalysts of this series decreases in the following order:

$$\text{Y} > \text{Ni} \approx \text{Mn} > \text{Cd} > \text{Zn}$$

According to the data presented in Fig. 4 more than 90% decomposition efficiency of N_2O can be achieved at 425 °C for Cu- and Fe-ZSM-5 and at 475 °C for Co-ZSM-5 catalysts. The higher activity exhibited by Cu-, Fe- and Co-ZSM-5 catalysts is in agreement with the literature data for the catalysts prepared via other routes [1,4,31,41,80–86]. Among the available literature data only few papers concerned with the comparison between the activities of the different metals exchanged zeolites (see for example refs. [4,80,81], where the comparison was reported for catalysts prepared via ion-exchange from solution only). In this regard, Li and Armor [80] reported the order Cu > Co > Fe. This order is in contrast with our results (Fig. 4a).

Inspection of Figs. 2 and 4 and the acidity data presented in Table 2 reveals that the activity variation of the different M-ZSM-5 catalysts cannot be related to the variation of Lewis and/or Brnøsted acidity. In other words, there is no clear correlation between the cation type utilized and both the acidity of the tested catalysts and their activity in direct N_2O decomposition. This result is in accordance with already published statement for steam activated Fe-ZSM-5 catalysts that, the role of Brønsted and Lewis acidic sites does not seem to be crucial for N_2O activation and decomposition, since steam treatment diminishes the concentration of strong acid sites appreciably, while the activity increases [86]. The micropore surface area measurements of some of the catalysts under investigation (Table 2) show significant changes with the variation of the metal cation. This is also true for the micropore volumes. In this context, the estimated pore volume of Fe-ZSM-5 is 0.161 $cm^3\,g^{-1}$ which is close to that obtained for H-ZSM-5 (0.177 $cm^3\,g^{-1}$). The other catalysts show lower micropore volume; however, all the values reported here are higher than 0.1 $cm^3\,g^{-1}$. This reflects that the pores in all the catalysts remain accessible, a fact which reflect that the activity change in the N_2O decomposition cannot also be anticipated to some textural changes. Moreover, possible effects caused by structural changes are also unlikely because the MFI structure remains intact as it was judged from the XRD analysis.

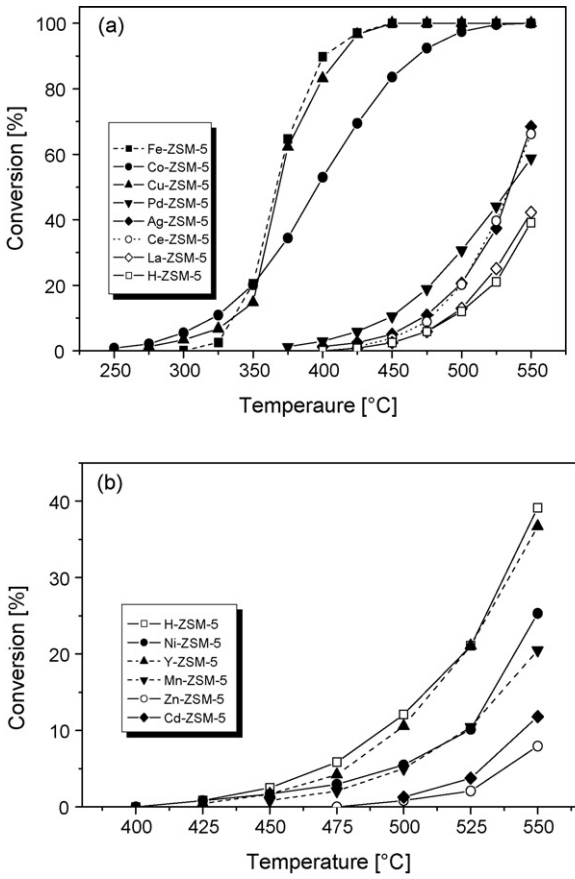

Fig. 4. Dependence of N_2O conversion % on the reaction temperature of the different transition metal exchanged ZSM-5 zeolite catalysts as well as the parent H-ZSM-5 (exchange level 100%, Si/Al = 25). Conditions: 500 ppm N_2O in He; total flow, 125 $cm^3\ min^{-1}$; weight of catalyst, 0.5 g.

In situ electrical conductivity measurement is considered as an interesting tool for the investigation of gas–solid and solid–solid interactions. However, very few electrical studies have been reported for the catalytic decomposition of nitrogen oxides [87–89]. Wagner [87] observed an electrical conductivity decrease of zinc oxide in the presence of N_2O. Dell et al. [88] correlated the N_2O decomposition activity for a series of metal oxides with their semiconductivity properties. According to their classification, p-type oxides are most active, n-type the least, and insulators are intermediate. In situ electrical conductivity was also reported for the NO decomposition over $V_2O_5/WO_3/TiO_2$ catalyst [89]. Due to the lack of information about the conductivity variation up on the admission of N_2O over zeolites, we decided to conduct some in situ electrical conductivity measurements in the presence of nitrous oxide in a trial to get information on the solids under conditions close to that of catalysis. The obtained results, upon admission of 500 ppm N_2O at 500 °C, are represented in Fig. 5 as log (σ/σ_0) versus time for the various transition metal exchanged ZSM-5 catalysts. The general feature of all the catalysts is a decrease in their corresponding relative conductivity values with time. The order of conductivity decrease is similar to that observed during the catalytic measurements (Fig. 4). In other words, the catalysts under investigation can also be divided into two groups based on their magnitude of the conductivity decrease; (i) group (A), which exhibits higher conductivity decrease compared to the H-ZSM-5. This group includes Fe-, Co-, Cu-, Pd-, La-, Ce- and Ag-ZSM-5 catalysts. (ii) Group (B), on the other hand, includes Ni-, Mn-, Cd-, Zn-, and Y-ZSM-5 catalysts which are characterized by only a mild

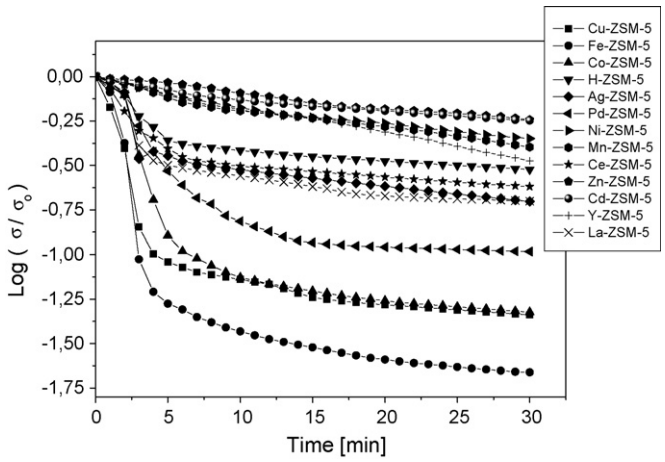

Fig. 5. Variation of the log (σ/σ_0) with time for the different transition metals exchanged ZSM-5 catalysts up on N_2O admission. Conditions: 500 ppm N_2O in N_2; total flow, 200 $cm^3\ min^{-1}$; weight of catalyst, 0.5 g.

conductivity decrease. The conductivity decreases abruptly in the first five minuets then gradually for group (A), whereas group (B) catalysts exhibit continuous mild decrease in the whole time scale.

The decrease in the conductance of the different catalysts under investigation in the presence of N_2O in the feed indicates that, the catalytic reaction is controlled by electronic functions, where the ease with which an electron can be transported from the bulk seems to be of great importance in determining the extent of adsorption process. Let us consider the nitrous oxide decomposition mechanism. Generally, there are two principal mechanisms; the first one involves dissociative electron transfer [87,88,90,91], whereas the second one deals with oxygen atom transfer [91,92]. The steps involved in the first mechanism can be summarized as follows:

$$N_2O_{(g)} + e^- \rightarrow N_2O^-{}_{(ads.)} \quad (2)$$

$$N_2O^-{}_{(ads.)} \rightarrow N_{2(g)} + O^-{}_{(ads.)} \quad (3)$$

$$2O^-{}_{(ads.)} \rightarrow O_{2(g)} + 2e^- \quad (4)$$

In this mechanism, ionosorption of N_2O via electron capture (Eq. (2)) will cause a consumption of the charge carriers and, thus, decreases the electrical conductivity. Similar argument was suggested for the NO adsorption [89]. The removal of surface lattice oxygen (Eq. (4)) will cause an increase of the electrical conductivity as a result of increasing the number of charge carriers. Eq. (2) is plausible since N_2O has positive electron affinity ranging from 0.3 to 0.8 eV [93]. Moreover, spectral behaviour and characteristics of adsorbed N_2O on chromia rule out the existence of N_2O^- species [94]. The formation of O^- species (Eq. (3)) was confirmed by ESR studies during N_2O decomposition over CoO-MgO catalysts [95] and discussed by other authors for N_2O decomposition over Fe-ZSM-5 [96]. Based on DFT modelling combined with computational spectroscopy [91], it was found that the N–N–O bond bending is imperative not only for triggering the electron transfer, yielding through N_2O^- transient the key O^- intermediate, but also for the energetic feasibility of this process.

From the inspection of the data presented in Fig. 5, and based on the above discussion, the following points could be raised: (i) during the first 5–10 min, the rate of reaction (2) over group (A) catalysts is higher than that of reaction (4). With further increase in time the rate of reaction (4) increases and after about 30 min close rates could be suggested. On the other hand, over group (B)

catalysts, it seems that reaction (4) proceeds with a lower rate than that of reaction (2). This, in turn, suggests that oxygen desorption over the group (A) catalysts is easier than that over group (B) ones; (ii) from the higher conductivity decrease observed on group (A) catalysts (specially in case of Co-, Cu-, and Fe-ZSM-5 catalysts), it is plausible to suggest that there are substantially more charge carriers on group (A) catalysts than on the group (B) ones. This could be correlated with the process know as auto-reduction. In this process, part of the Cu^{2+}, Fe^{3+} are reduced to Cu^{+} or Fe^{2+} by treatment in vacuum or inert atmosphere at high temperature with the release of H_2O and O_2 [97,98]. For example, in case of copper-containing zeolite, the following routes were suggested:

$$2[CuOH]^{+} \rightarrow H_2O + Cu^{+} + [Cu^{2+}O^{-}]^{+} \rightarrow 2Cu^{+} + \tfrac{1}{2}O_2 \quad (5)$$

$$2[CuOH]^{+} \rightarrow H_2O + [Cu^{2+}{-}O^{-}{-}Cu^{2+}]^{2+} \rightarrow 2Cu^{+} + \tfrac{1}{2}O_2 \quad (6)$$

Accordingly, from the amplitude of the conductivity decrease, one may conclude that Fe-ZSM-5 contains higher concentration of these reduced sites whereas Co- and Cu-ZSM-5 catalysts seem to have approximately close concentrations. Thus, we can relate the higher activity of group (A) catalysts to the higher reduced site formed during the heat pre-treatment. This is in a good agreement of the reported work of Pringruber et al. [33,38] who reported that the steady-state activity of Fe-ZSM-5 catalysts towards N_2O direct decomposition correlates well with the concentration of Fe^{2+} sites created by autoreduction at 600 °C.

3.3.2. N_2O decomposition over Co-, Cu- and Fe-ZSM-5 catalysts

Since Co-, Cu- and Fe-ZSM-5 catalysts unquestioningly reveal the highest N_2O conversion among all catalysts under investigation, hence further experiments were carried out in order to address the factors affecting their catalytic activity, namely (a) Si/Al ratio, (b) exchange level, (c) calcination temperature, and (d) milling time. In this context, it is worth mentioning that some of our cobalt as well as copper-containing catalysts exhibited an oscillation phenomenon, a property that will be discussed in forthcoming papers.

3.3.2.1. Si/Al ratio. Fig. 6 shows the dependence of the turnover frequencies (TOFs) for Co-, Cu-, and Fe-ZSM-5 catalysts on the Si/Al ratio. The TOF is defined as the mole of N_2O per second per mole of metal (ICP determined) contained in the different catalysts, where the M/Al ratio was adjusted to reach a value of 0.5. It is evident that the three series of catalysts behave differently, for Co-ZSM-5 catalysts increasing the Si/Al ratio from 25 to 200 is accompanied by a continuous increase in the TOF values till Si/Al range of 100–150, then the TOF values decrease for Si/Al = 200. However, at reaction temperature 550 °C the TOF increase continuously with the Si/Al increase. Such continuous TOF increase represents the general trend of Cu-ZSM-5 catalysts at temperatures ≥400 °C. Fe-ZSM-5 series shows a mild TOF decrease as the Si/Al increases from 25 to 40. This is followed by a continuous TOF increase till Si/Al range of 100–150 which is followed a sharp decrease for the catalyst with Si/Al = 200. Noteworthily, the highest TOFs are obtained for Cu-ZSM-5 with Si/Al of 200 all over the tested reaction temperatures. These results further emphasize the severe role of Si/Al ratio and the metal type during the direct N_2O decomposition. We can compare the TOF values obtained for the catalysts presented in Fig. 6 (for the catalysts with Si/Al = 40) with those reported by Kapteijn et al. [81] for Co-, Cu-, and Fe-ZSM-5 (Si/Al = 37.2 prepared by ion exchange from solution and calcined at 650 °C). It appears that a similar activity order, Cu > Co > Fe, can be observed. In comparison with precious metals exchanges zeolites, Chang et al. [99] reported a TOFs (mmol N_2O $Ru^{-1}S^{-1}$) of 0.513 at 200 °C and 0.148 at 280 °C during N_2O decomposition over Ru-HNaUSY and Ru-NaZSM-5 zeolites, respectively. Undoubtedly, these values are higher than those presented here (Fig. 6) irrespective of the Si/Al ratio.

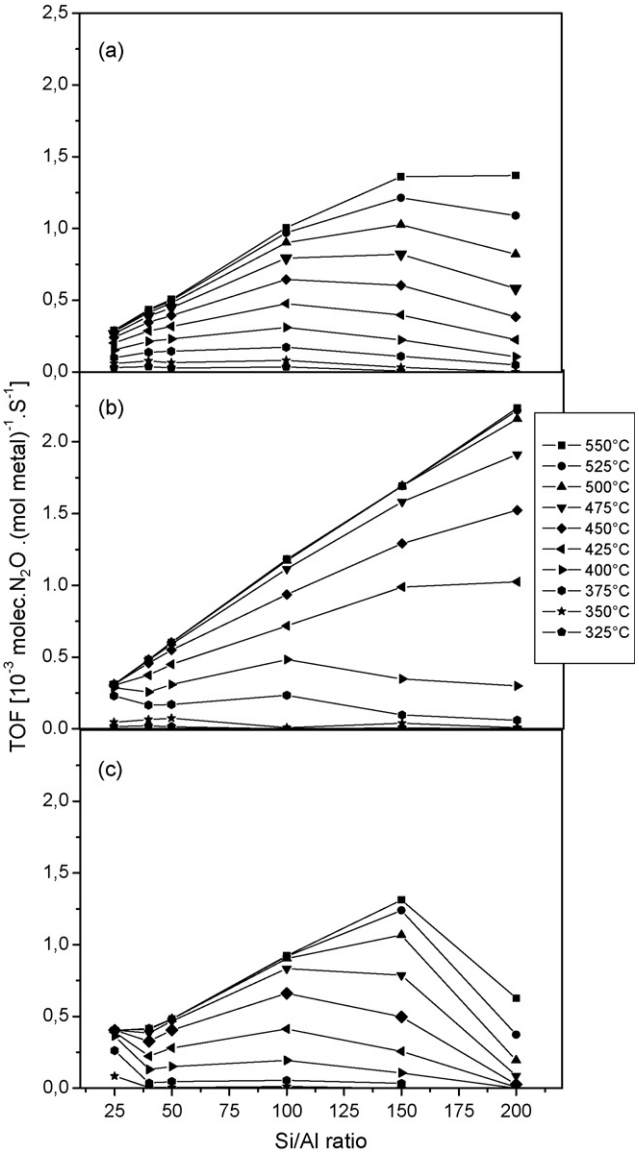

Fig. 6. Dependence of N_2O TOFs on the Si/Al ratio at different temperatures for Co-ZSM-5 (a), Cu-ZSM-5 (b) and Fe-ZSM-5 (c) catalysts (M/Al = 0.5). Conditions: 500 ppm N_2O in He; total flow, 125 cm^3 min^{-1}; weight of catalyst, 0.5 g.

3.3.2.2. Exchange level. In the open literature there are many reports dealing with the effect of ion-exchange level on the activity towards N_2O removal. Kögel et al. [50] have reported that increasing the exchange level of Fe-ZSM-5 (Si/Al = 11.4, prepared by SSIE) from 25 up to 150% is accompanied by a continuous increase in its activity towards N_2O reduction with propane in the presence of NO. In agreement, Pophal et al. [79] have also demonstrated that increasing the exchange level of Fe-ZSM-5 (Si/Al = 11.7, prepared by ion-exchange from aqueous solution) from 20 to 80% is also resulted in a continuous increase in N_2O reduction with propene. For the same catalyst, i.e. Fe-ZSM-5 (Si/Al = 12.5, prepared by ion-exchange from aqueous solution), a third research group [41] reported that the exchange level does not affect its activity in N_2O direct decomposition and in SCR of N_2O with NH_3. On Cu-ZSM-5 [100] and Co-ZSM-5 [80], prepared also via the

conventional ion-exchange from aqueous solutions, increasing the M/Al ratios produces a continuous increase in direct N_2O decomposition activity. In the above-mentioned investigations there is a lack of information concerned with a comparative study for the effect of increasing the exchange level for Co-, Cu- and Fe-ZSM-5 catalysts prepared via SSIE route. Thus, our experiments were extended to check the effect of increasing the ion-exchange levels for the two end-members of the catalysts presented in Fig. 6, i.e. for the catalysts with Si/Al = 25 and 200. The obtained data for Co-, Cu- and Fe-catalysts with Si/Al ratios of 25 and 200 are presented in Figs. 7 and 8, respectively. A sigmoid type conversion–temperature curves can be observed for all the catalysts presented in Fig. 7. In addition, the onset of the reaction is shifted towards lower temperatures as a result of increasing the exchange level

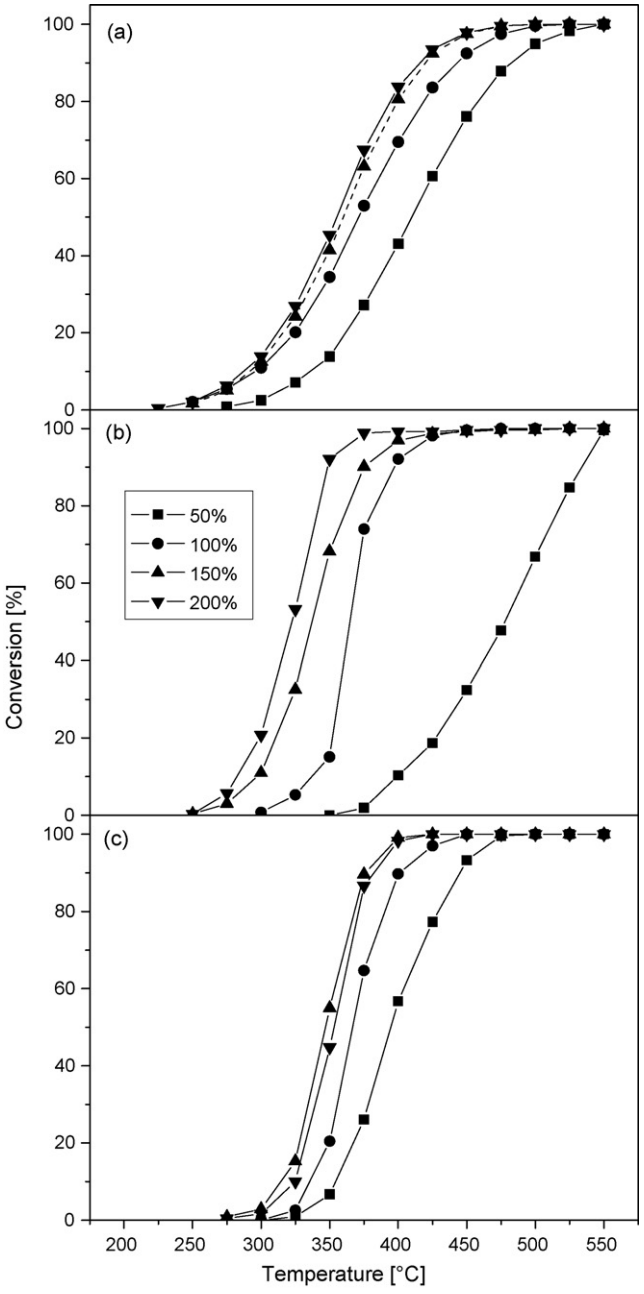

Fig. 7. Conversion of N_2O versus temperature obtained for Co-ZSM-5 (a), Cu-ZSM-5 (b) and Fe-ZSM-5 (c) catalysts at 50–200% exchange levels (Si/Al = 25). Conditions: 500 ppm N_2O in He; total flow, 125 cm^3 min^{-1}; weight of catalyst, 0.5 g.

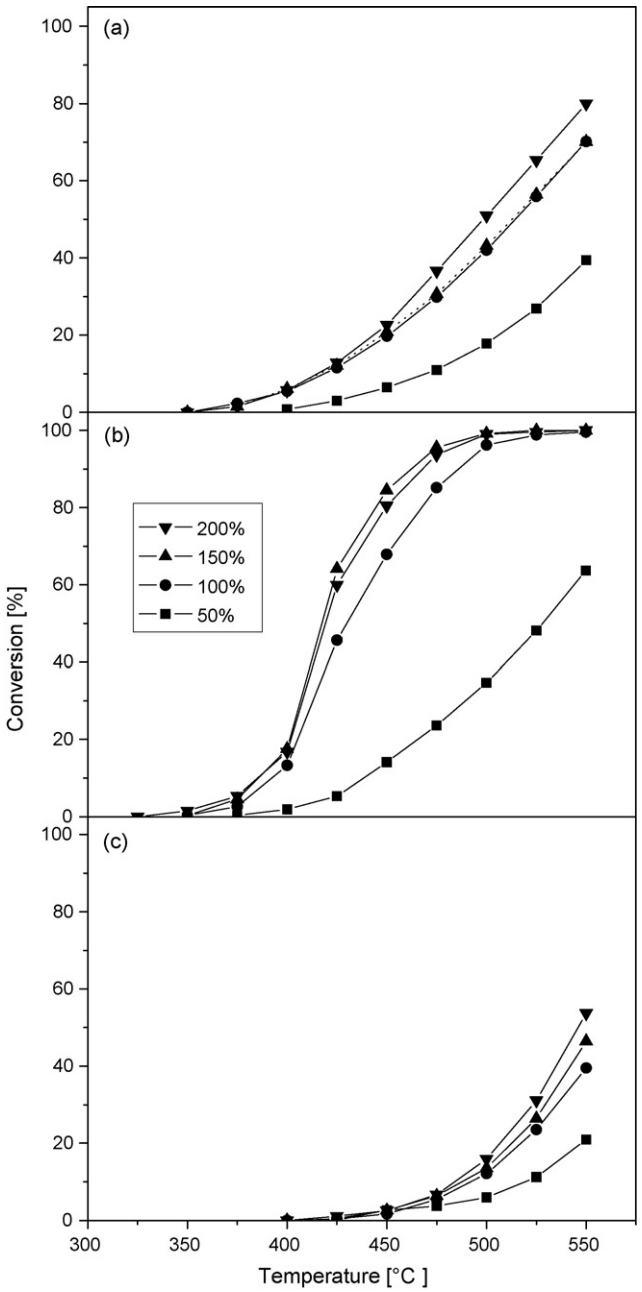

Fig. 8. Conversion of N_2O versus temperature obtained for Co-ZSM-5 (a), Cu-ZSM-5 (b) and Fe-ZSM-5 (c) catalysts at 50–200% exchange levels (Si/Al = 200). Conditions: 500 ppm N_2O in He; total flow, 125 cm^3 min^{-1}; weight of catalyst, 0.5 g.

from 50 to 200%. Such effect is much more pronounced in case of Cu-ZSM-5 catalysts. Increasing the exchange levels up to 200% is accompanied with a continuous shift of the conversion values towards lower temperatures for Co- and Cu-ZSM-5 catalysts, whereas a slight decrease in the activity is obtained on raising the exchange level from 150 to 200% for Fe-ZSM-5 catalyst. Interestingly, copper-containing catalysts showed the lowest and the highest activity patterns among the three cations for the 50 and 200% exchange levels, respectively.

Regarding the catalysts with Si/Al = 200 (Fig. 8), it is evident that the onset of the reaction starts at about 350, 375 and 425 °C for Cu-, Co- and Fe-ZSM-5 catalysts, respectively. In addition, increasing the exchange level yields a continuous increase in the N_2O decomposition activities, meanwhile Co-ZSM-5 catalyst

with 100 and 150% exchange levels exhibit approximately similar conversion values. A sigmoid shape can be observed in the conversion–temperature curves only for Cu-catalysts with exchange level ≥100%. Comparing the relevant catalysts in the three series (Fig. 8a–c) reveals the following activity order:

Cu > Co > Fe

Matching the data presented in Figs. 7 and 8 manifests that, Co- and Fe-ZSM-5 catalysts with Si/Al = 200 (for all exchange levels tested) have lower activities than the corresponding ones with Si/Al = 25 and 50% exchange level. On the other hand, Cu-ZSM-5 catalyst with Si/Al = 200 and a sigmoid conversion–temperature curves are more active than that with Si/Al = 25 and 50% exchange level. The trend N_2O decomposition activity increase as a result of M/Al increase shown in Fig. 8 is a direct response to the results presented in Fig. 6, where Cu-ZSM-5 catalyst exhibited the highest TOFs than Co- or Fe-ZSM-5 ones. In this context, Rakić et al. [101] have investigated N_2O and CO adsorption behaviour of Cu-, Co-, and Fe-under-exchanged ZSM-5 catalysts (Si/Al = 20) using microcalorimetry and infrared spectroscopy. Their results revealed that Cu-ZSM-5 shows significantly better performance than Co- or Fe-ZSM-5. In addition, nitrous oxide can be chemisorbed over Cu-ZSM-5. Accordingly, one can arrive at the conclusion that neither the total number of active sites which can be created by aluminium framework ion, nor the ion-exchanged cations affect the activity alone.

3.3.2.3. Calcinations temperature. The study was, then, devoted to check the effect of increasing the calcinations temperature (up to 650 °C) on the N_2O decomposition activity for Co-, Cu- and Fe-ZSM-5 catalysts. The obtained results were plotted in Fig. 9 for the samples with Si/Al = 25 and exchange levels of 50 and 200%. Two points could be raised from inspection of Fig. 9: (i) a retarding effect can be observed as a result of pushing the calcinations temperature from 550 to 650 °C for Co- and Cu-ZSM-5 catalysts. This effect is much more pronounced for Cu-ZSM-5 with 50% exchange level. (ii) An enhancement effect is observed for Fe-ZSM-5 catalyst with 50% exchange level. Meanwhile, increasing the iron content in this catalyst (to 200%) was not affected by the calcinations temperature raise.

It is well agreed in the literature that Cu-ZSM-5 catalysts contain Cu_2O_2 clusters known as bis(μ-oxo) dicopper core which have a diagnostic UV–vis band at 22 700 cm^{-1} [35,102–104]. Such species was reported to play a vital rule in the decomposition of NO [35,102] as well as N_2O [35] via controlling the release of oxygen. Moreover, these cores show a remarkable activity towards methane to methanol conversion [103]. The bis(μ-oxo)dicopper core was also reported to be EPR silent [102].

It has been demonstrated that, the presence of the bis(μ-oxo)dicopper cores in the zeolites is influenced by many factors, namely the exchange level, Si/Al ratio, calcination temperature, and zeolite topology [103]. The optimal calcination temperature region lies between 450 and 650 °C [103]. Calcining the Cu-ZSM-5 at higher temperatures led to an irreversible loss of the capability to stabilize these Cu_2O_2 cores in the MFI structure [103]. The 22,700 cm^{-1} band is only found for the Cu/Al ratio > 0.2 [103,104], meanwhile its intensity is maximum for the catalysts having Si/Al in the range 12–30 (Cu/Al ≈ 0.5), while for the samples with higher Si/Al ratio (77 and 120) the intensity of this band is drastically decreased [103]. In other words, the optimal Si/Al ratio for the stabilization of the bis(μ-oxo)dicopper core is between 12 and 30.

In the light of these interesting literature data one may understand the behaviour of Cu-ZSM-5 catalysts (shown in Fig. 9) in terms of the presence of the bis(μ-oxo)dicopper cores. In this way, the higher activity of the 200% exchanged catalyst compared

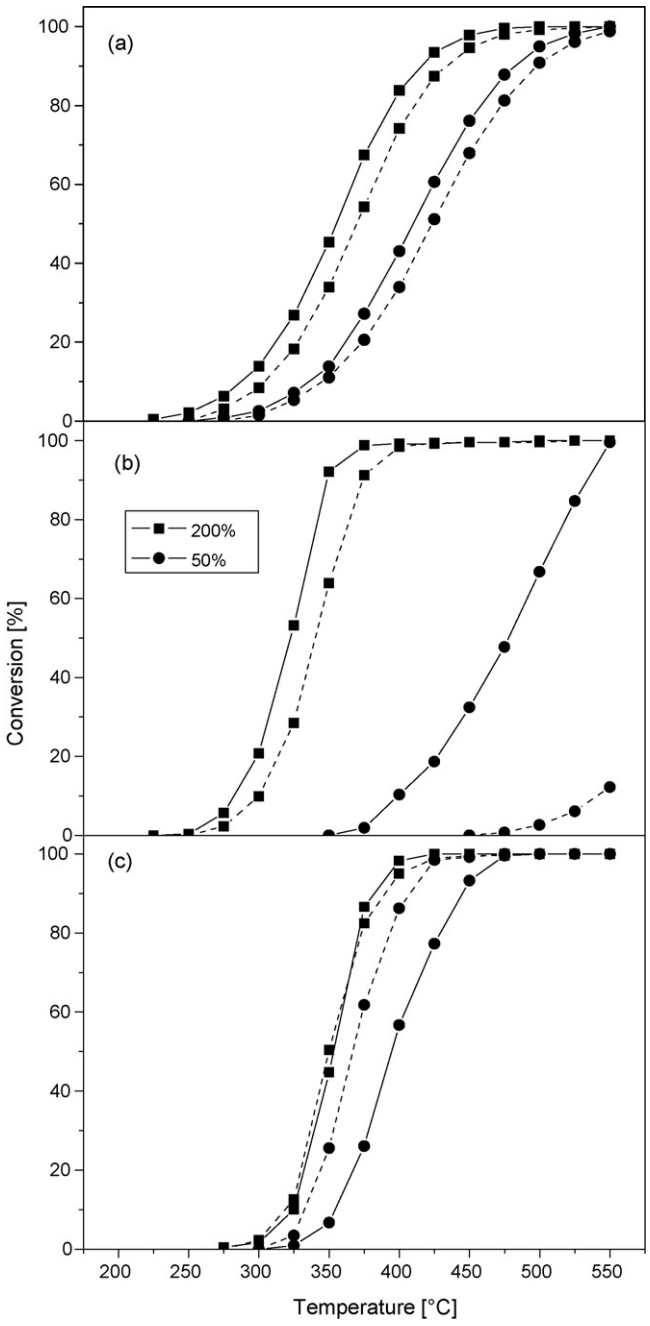

Fig. 9. Effect of calcination temperature on conversion of N_2O obtained for Co-ZSM-5 (a), Cu-ZSM-5 (b) and Fe-ZSM-5 (c) catalysts (Si/Al = 25, exchange levels of 50 and 200%). The solid curves represent the catalysts calcined at 550 °C whereas the dashed ones represent the catalysts calcined at 650 °C. Conditions: 500 ppm N_2O in He; total flow, 125 cm^3 min^{-1}; weight of catalyst, 0.5 g.

to that of the 50% exchanged one (calcined at 550 °C) is due to the expected increased amounts of the bis(μ-oxo)dicopper cores. In agreement, the sudden increase in the N_2O decomposition activity over Cu-ZSM-5 was observed upon increasing Cu/Al ratio from 0.22 to 0.29 was attributed, to the increasing number of bis(μ-oxo)dicopper cores [35]. On raising the calcinations temperature to 650 °C (Fig. 9), the 200% exchange catalyst showed a mild activity decrease whereas the 50% exchanged one exhibits a sharp decrease in the activity. This also indicates that active sites for this reaction, bis(μ-oxo)dicopper cores, suffer a more pronounced decrease upon increasing the calcinations temperature for the lower Cu/Al catalysts.

XRD diffractograms reveal the presence of minor amounts of hematite (JCPDS card no. 86–550) for the 200% exchanged sample, being calcined at 550 °C (not shown). The amount of hematite increases with increasing the calcinations temperature to 650 °C. In this regard, the presence of hematite was previously detected in samples with a Fe(II)/Al ratio above 0.5 for Fe-ZSM-5, Si/Al = 11.4, catalysts prepared by the SSIE method [40]. One possibility for the formation of the iron oxide is that during ion exchange small particles of $FeCl_2$ are nucleated within the pores of the zeolites, which is transformed to FeO_x upon hydrolysis [105]. Another route for the formation of FeO_x might be the drying period in the presence of air [106]:

$$FeCl_2 \cdot 4H_2O + \text{H-ZSM-5} \overset{\text{air}/550^\circ\text{C}}{\longrightarrow} \text{FeCl-ZSM-5} + 4H_2O + HCl \quad (7)$$

$$2\text{FeCl-ZSM-5} + H_2O \overset{\text{washing/drying}}{\longrightarrow} \text{Fe-ZSM-5} + FeO_x + 2HCl \quad (8)$$

Several research groups have shown that high-temperature calcination (600–700 °C) enhances the N_2O decomposition [36,37,39,68], methane–methanol [107] and benzene–phenol [108] conversion over Fe-ZSM-5 catalysts. Panov's group suggested that, the active sites for the N_2O decomposition over Fe-ZSM-5 is the so called α sites [109–111]. Such sites were proposed to consist of binuclear Fe centers [63]. It has been reported that, these sites are created upon high-temperature activation leading to reduction of some Fe^{3+} species to Fe^{2+} [96,112]. The work of Hensen et al. [68] has demonstrated that, the amount of these active sites correlates to the amount of Fe^{2+} as probed by ^{57}Fe Mössbauer spectroscopy at 4.2 K. In view of this literature data, we may conclude that high-temperature treatment led only to an increase of the number of sites able to decompose nitrous oxide at relatively low temperatures on the 50% exchanged sample. On the other hand, the positive effect of the high temperature treatment of the other sample, 200%, is limited due to the increased formation of the iron oxide. Such phase was shown to be inactive towards N_2O direct decomposition [40].

According to the work of Wichterlová group [58,113,114], Co^{2+} ions in the ZSM-5 can occupy three types of positions: α at the main channels and represents two five member rings forming the six-member ring on the channel wall, β at the deformed six-member rings at the intersections of the straight and sinusoidal channels, and γ which is located at the sinusoidal channels. Recently, Chupin et al. [115] demonstrated that, when the degree of exchange is >60%, Co^{2+} ions are preferentially located in α sites. At low degrees of exchange < 60%, cations in α sites might migrate to β positions depending on the temperature [115]. A literature survey revealed a lack of information concerning the influence of increasing the calcinations temperature on N_2O decomposition activity over Co-ZSM-5. From the results depicted in Fig. 9, it appears that raising the calcination temperature till 650 °C is accompanied by a mild decrease in the N_2O decomposition activity for the under- as well as the over-exchanged catalysts. In other words, irrespective of the position of cobalt in the MFI structure, increasing the calcination temperature leads to a decrease in the catalytic activity.

3.3.2.4. Milling time. Utilizing the SSIE method in the preparation of active M-ZSM-5 catalysts bears out an interesting question; does the milling time affect the activity of the produced catalysts. To answer this question series of experiments were carried out applying a milling durations of 30 min and 4 h for Co-, Cu- and Fe-ZSM-5 catalysts having Si/Al ratio of 25 and 200% exchange level. The obtained results were plotted in Fig. 10 together with those obtained with 1 h milling time, i.e. with the catalysts already presented in Fig. 7 with Si/Al = 25 and 200% exchange level. Changing the milling time yields parallel curves in case of both Co- and Fe-ZSM-5 catalysts. Meanwhile, intercepted curves can be observed for Cu-ZSM-5 catalyst. It is obvious that 1 h milling gives an optimum activity in case of Co-ZSM-5 catalyst. The activity of copper-containing catalyst seems to be independent on the milling time. For Fe-ZSM-5, increasing the milling time to 4 h produces a shift of the activity curves towards higher temperatures. Fig. 11 shows the XRD patterns of the Co-, Cu- and Fe-ZSM-5 catalysts (Si/Al = 25 and 200% exchange level) subjected to different milling times. Inspection of this figure reveals the presence of trace amounts of Co_3O_4, CuO and Fe_2O_3 in their corresponding diffractograms. Q_{Al} values were used as a relative measure of the crystallinity variation as a result of increasing the milling time. Such values were calculated by comparing the XRD intensities of the different catalysts shown in Fig. 11 with those of the reference diffractogram of aluminum oxide α-Al_2O_3 (corundum). Detailed information about the calculation of Q_{Al} is given elsewhere [18]. Table 3 lists the calculated Q_{Al} values of the catalysts under investigation being subjected to different milling time durations.

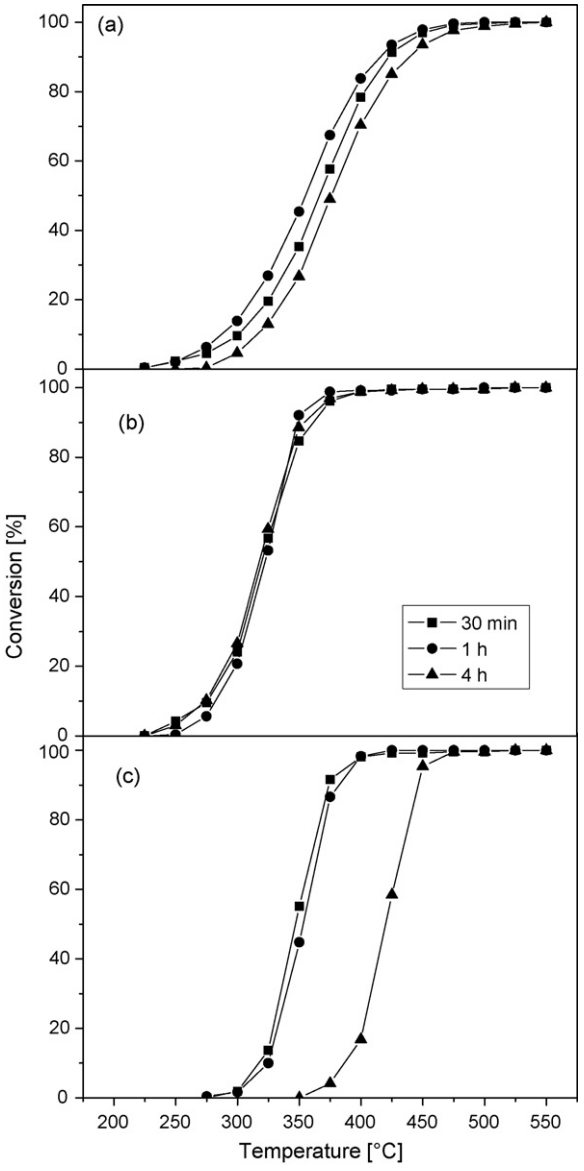

Fig. 10. Dependence of N_2O conversion % on the reaction temperature for Co-ZSM-5 (a), Cu-ZSM-5 (b) and Fe-ZSM-5 (c) catalysts applying different milling times (Si/Al = 25, 200% exchange level). Conditions: 500 ppm N_2O in He; total flow, 125 $cm^3\ min^{-1}$; weight of catalyst, 0.5 g.

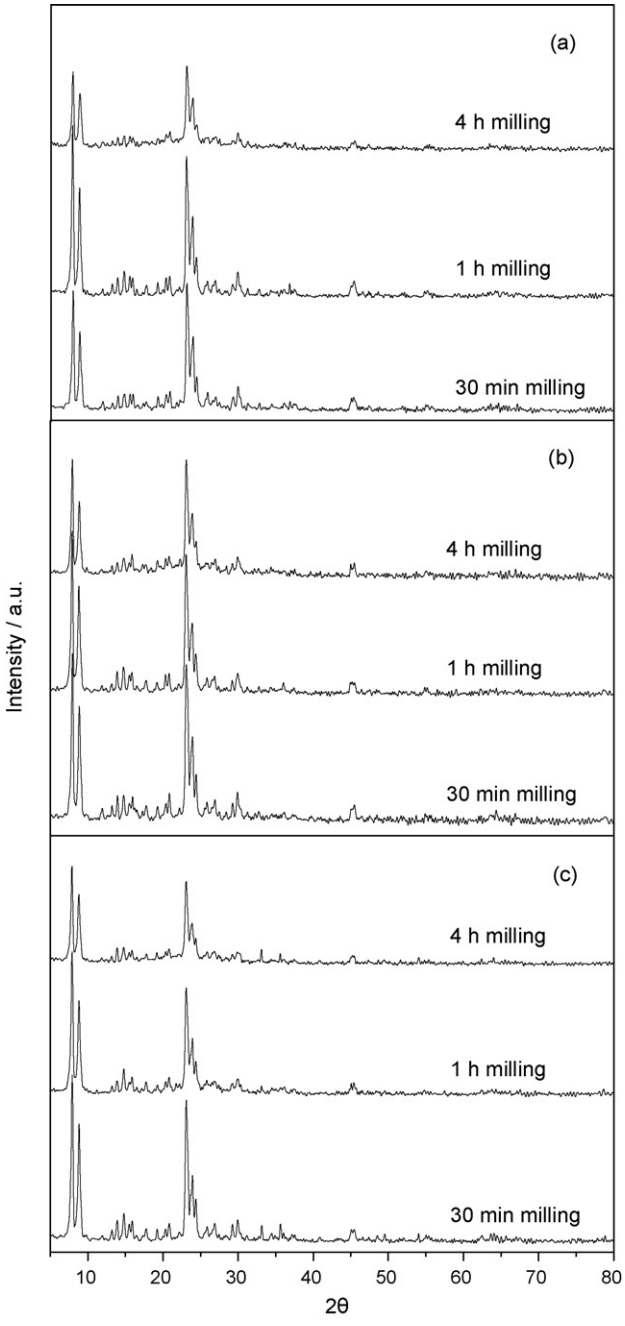

Fig. 11. XRD patterns obtained for Co-ZSM-5 (a), Cu-ZSM-5 (b) and Fe-ZSM-5 (c) catalysts applying different milling times (Si/Al = 25, 200% exchange level).

Table 3
Variation of the crystallinity, expressed in terms of Q_{Al} values, of Co-, Cu-, and Fe-ZSM-5 catalysts (Si/Al = 25) with milling time

Milling time [h]	Calculated Q_{Al} values[a]		
	Co-ZSM-5	Cu-ZSM-5	Fe-ZSM-5
0	0.98	0.98	0.98
0.5	0.82	1.03	0.91
1	0.86	0.90	0.69
4	0.54	0.78	0.53

[a] Q_{Al} values were calculated according to ref. [18].

One can spot the fact that milling Co-ZSM-5 zeolite for 1 h yields a catalyst with higher Q_{Al} value compared to the Co-ZSM-5 catalysts milled at 30 min or 4 h. Moreover, it is evident that Co- and Fe-catalysts suffer from about 44 and 46% loss in the crystallinity, respectively, as a result of increasing the milling time to 4 h. Under the same milling treatment, Cu-ZSM-5 catalyst showed only about 20% crystallinity loss. Accordingly, the trend of activity variation observed as a result of changing the milling time of the Co-, Cu-, and Fe-ZSM-5 catalysts could be related to the crystallinity variation of such catalysts.

4. Conclusions

A set of transition metal exchanged ZSM-5 zeolites has been prepared via solid-state ion-exchange (SSIE) method and was tested in N_2O direct decomposition. Based on pyridine adsorption measurements, a degree of ion exchange more than 60% was obtained. With respect to the catalytic activity, the prepared catalysts was divided into two groups: (i) the first one exhibits higher activity than H-ZSM-5, which includes Co-, Cu-, Fe-, Pd-, Ag-, Ce- and La-ZSM-5 catalysts, and (ii) the second group includes Ni-, Y-, Mn-, Zn-, and Cd-ZSM-5 catalysts, which has lower activity than H-ZSM-5. The higher activity of the first group catalysts, compared to the second group catalysts, was related to their higher ability to undergo reduction during the heat pre-treatment. Comparative studies have been performed over Cu-, Fe- and Co-ZSM-5 catalysts since they showed the highest activity patterns among all the tested zeolites. Changing Si/Al ratio as well as the exchange level led us to conclude that neither the total number of active sites which can be created by aluminium framework ions, nor the ion-exchanged cations affect the activity alone. Moreover, it was shown that the N_2O decomposition activity over such series of catalysts is sensitive to the calcinations temperature as well as the milling time.

Acknowledgements

B.M. Abu-Zied thanks the financial support from the Deutscher Akademischer Austausch Dienst (DAAD) and Bayerische Forschungsstiftung during his research visits to Germany. The grant awarded to W. Schwieger from the DAAD during his research visit to Egypt is also acknowledged. W. Schwieger would like to thank VCI and DFG for the chemicals and equipments support.

References

[1] G. Centi, S. Perathoner, F. Vazzana, M. Marella, M. Tomaselli, M. Mantegazza, Adv. Environ. Res. 4 (2000) 325–338.
[2] M.K.K. Khalil, Chemosphere-Global Change Sci. 2 (2000) 233.
[3] F. Kapteijn, J. Rodriguez-Mirasol, J.A. Moulijn, Appl. Catal. B 9 (1996) 25–64.
[4] C.M. de Correa, A.L. Villa, M. Zapata, Catal. Lett. 38 (1996) 27–32.
[5] R. Pitchai, K. Klier, Catal. Rev. -Sci. Eng. 28 (1986) 13–88.
[6] K.S. Pillai, J. Jia, W.M.H. Sachtler, Appl. Catal. A 264 (2004) 133–139.
[7] D. Meloni, R. Monaci, V. Solinas, G. Berlier, S. Bordiga, I. Rossetti, C. Oliva, L. Forni, J. Catal. 214 (2003) 169–178.
[8] L.V. Pirutko, V.S. Chernyavsky, A.K. Uriarte, G.I. Panov, Appl. Catal. A 227 (2002) 143–157.
[9] S. Perathoner, F. Pino, G. Centi, G. Giordano, A. Katovic, J.B. Nagy, Top. Catal. 23 (2003) 125–136.
[10] A. Ribera, I.W.C.E. Arends, S. de Vries, J. Pérez-Ramírez, R.A. Sheldon, J. Catal. 195 (2000) 287–297.
[11] G. Centi, S. Perathoner, R. Arrigo, G. Giordano, A. Katovic, V. Pedulá, Appl. Catal. A 307 (2006) 30–41.
[12] I. Yuranov, D.A. Bulushev, A. Renken, L. Kiwi-Minsker, Appl. Catal. A 319 (2007) 128–136.
[13] V.N. Parmon, G.I. Panov, A. Uriarte, A.S. Noskov, Catal. Today 100 (2005) 115–131.
[14] G. Centi, S. Perathoner, F. Pino, R. Arrigo, G. Giordano, A. Katovic, V. Pedulá, Catal. Today 110 (2005) 211–220.
[15] J.B. Taboada, E.J.M. Hensen, I.W.C.E. Arends, G. Mul, A.R. Overweg, Catal. Today 110 (2005) 221–227.

[16] E.J.M. Hensen, Q. Zhu, R.A.J. Janssen, P.C.M.M. Magusin, P.J. Kooyman, R.A. van Santen, J. Catal. 233 (2005) 123–135.
[17] E.J.M. Hensen, Q. Zhu, R.A. van Santen, J. Catal. 233 (2005) 136–146.
[18] J. Kanellopoulos, A. Unger, W. Schwieger, D. Freude, J. Catal. 237 (2006) 416–425.
[19] J.A.Z. Pieterse, S. Booneveld, R.W. van den Brink, Appl. Catal. B 51 (2004) 215–228.
[20] J. Pérez-Ramírez, F. Kapteijn, G. Mul, J. Moulijn, Appl. Catal. B 35 (2002) 227–234.
[21] A. Wącław, K. Nowińska, W. Schwieger, A. Zielińska, Catal. Today 90 (2004) 21–25.
[22] A. De Stefanis, M. Dondi, G. Perez, A.A.G. Tomlinson, Chemosphere 41 (2000) 1161–1165.
[23] K. Sun, H. Xia, E. Hensen, R. van Santen, C. Li, J. Catal. 238 (2006) 186–195.
[24] A.H. Øygarden, J. Pérez-Ramírez, Appl. Catal. B 65 (2006) 163–167.
[25] I. Melián-Cabrera, S. Espinosa, J.C. Groen, B. v/d Linden, F. Kapteijn, J.A. Moulijn, J. Catal. 238 (2006) 250–259.
[26] J.C. Groen, A. Brückner, E. Berrier, L. Maldonado, J.A. Moulijn, J. Pérez-Ramírez, J. Catal. 243 (2006) 212–216.
[27] B.M. Abu-Zied, Appl. Catal. A 334 (2008) 234–242.
[28] S. Alini, F. Basile, S. Blasioli, C. Rinaldi, A. Vaccari, Appl. Catal. B 70 (2007) 323–329.
[29] L. Xue, C. Zhang, H. He, Y. Teraoka, Appl. Catal. B 75 (2007) 167–174.
[30] C. Ohnishi, K. Asano, S. Iwamoto, K. Chikama, M. Inoue, Catal. Today 120 (2007) 145–150.
[31] D.A. Bulushev, L. Kiwi-Minsker, A. Renken, J. Catal. 222 (2004) 389–396.
[32] G.D. Pirngruber, L. Frunz, J.A.Z. Pieterse, J. Catal. 243 (2006) 340–349.
[33] G.D. Pirngruber, M. Luechinger, P.K. Roy, A. Cecchetto, P. Smirniotis, J. Catal. 224 (2004) 429–440.
[34] V. Barišić, F. Klingstedt, A. Naydenov, P. Stefanov, P. Kilpinen, M. Hupa, Catal. Today 100 (2005) 337–342.
[35] P.J. Smeets, M.H. Groothaert, R.M. van Teeffelen, H. Leeman, E.J.M. Hensen, R.A. Schoonheydt, J. Catal. 245 (2007) 358–368.
[36] Q. Zhu, E.J.M. Hensen, B.L. Mojet, J.H.M.C. van Wolput, R.A. van Santen, Chem. Comm. (2002) 1232–1233.
[37] Q. Zhu, B.L. Mojet, R.A.J. Janssen, E.J.M. Hensen, J. van Grondelle, P.C.M.M. Magusin, R.A. van Santen, Catal. Lett. 81 (2002) 205–212.
[38] G.D. Pirngruber, P.K. Roy, R. Prins, J. Catal. 246 (2007) 147–157.
[39] K. Krishna, M. Makkee, Catal. Lett. 106 (2006) 183–193.
[40] M. Rauscher, K. Kesore, R. Mönnig, W. Schwieger, A. Tißler, T. Turek, Appl. Catal. A 184 (1999) 249–256.
[41] A. Guzmán-Vargas, G. Delahay, B. Coq, Appl. Catal. B 42 (2003) 369–379.
[42] B. Coq, M. Mauveyin, G. Delahay, S. Kieger, J. Catal. 195 (2000) 298–303.
[43] K. Sugawara, T. Nobukawa, M. Yoshida, Y. Sato, K. Okumura, K. Tomishige, K. Kunimori, Appl. Catal. B 69 (2007) 154–163.
[44] T.N. Angelidis, V. Tzitios, Appl. Catal. B 41 (2003) 357–370.
[45] M.N. Debbagh, A. Bueno-López, C.S. Martínez de Lecea, J. Pérez-Ramírez, Appl. Catal. A 327 (2007) 66–72.
[46] V. Boissel, S. Tahir, C.A. Koh, Appl. Catal. B 64 (2006) 234–242.
[47] K.S. Chang, H.-J. Lee, Y.-S. Park, J.-W. Woo, Appl. Catal. A 309 (2006) 129–138.
[48] M.S. Kumar, J. Pérez-Ramírez, M.N. Debbagh, B. Smarsly, U. Bentrup, A. Brückner, Appl. Catal. B 62 (2006) 244–254.
[49] T. Hirano, Y. Kazahaya, A. Nakamura, T. Miyao, S. Naito, Catal. Lett. 117 (2007) 73–78.
[50] M. Kögel, R. Mönnig, W. Schwieger, A. Tissler, T. Turek, J. Catal. 182 (1999) 470–478.
[51] M. Yoshida, T. Nobukawa, S. Ito, K. Tomishige, K. Kunimori, J. Catal. 223 (2004) 454–464.
[52] E. Ruiz-Martínez, J.M. Sánchez-Hervás, J. Otero-Ruiz, Appl. Catal. B 61 (2005) 306–315.
[53] O. Sánchez-Galofré, Y. Segura, J. Pérez-Ramírez, J. Catal. 249 (2007) 123–133.
[54] T. Nobukawa, K. Sugawara, K. Okumura, K. Tomishige, K. Kunimori, Appl. Catal. B 70 (2007) 342–352.
[55] T. Nobukawa, M. Yoshida, K. Okumura, K. Tomishige, K. Kunimori, J. Catal. 229 (2005) 374–388.
[56] T. Chakia, M. Araia, T. Ebinab, M. Shimokawabe, J. Mol. Catal. A 227 (2005) 187–196.
[57] E.V. Kondratenko, J. Pérez-Ramírez, Catal. Today 119 (2007) 243–246.
[58] D. Kaucký, A. Vondrová, J. Dědeček, B. Wichterlová, J. Catal. 194 (2000) 318–329.
[59] Y. Kuroda, M. Iwamoto, Top. Catal. 28 (2004) 111–118.
[60] H. Yahiro, M. Iwamoto, Appl. Catal. A 222 (2001) 163–181.
[61] J. Pérez-Ramírez, F. Kapteijn, G. Mul, J. Moulijn, J. Catal. 208 (2002) 211–223.
[62] M. Kögel, B.M. Abu-Zied, M. Schwefer, T. Turek, Catal. Commun. 2 (2001) 273–276.
[63] El.-M. El-Malki, R.A. van Santen, W.M.H. Sachtler, J. Catal. 196 (2000) 212–223.
[64] I.O.Y. Liu, N.W. Cant, M. Kögel, T. Turek, Catal. Lett. 63 (1999) 241–244.
[65] Y. Li, J.N. Armor, Appl. Catal. A 188 (1999) 211–217.
[66] K. Lázár, G. Pál-Borbély, H.K. Beyer, H.G. Karge, Stud. Surf. Sci. Catal. 91 (1995) 551–559.
[67] P.R. Chapman, R.H. Griffith, J.D.F. Marsh, Proc. R. Soc. (Lond.) 224 (1954) 419–426.
[68] E.J.M. Hensen, Q. Zhu, M.M.R.M. Hendrix, A.R. Overweg, P.J. Kooyman, M.V. Sychev, R.A. van Santen, J. Catal. 221 (2004) 560–574.
[69] C. Torre-Abreu, M.F. Ribeiro, C. Henriques, G. Delahay, Appl. Catal. B 12 (1997) 249–262.
[70] C. Descorme, P. Gélin, C. Lécuyer, M. Primet, Appl. Catal. B 13 (1997) 185–195.
[71] G. Koyano, S. Yokoyama, M.O. Misono, Appl. Catal. A 188 (1999) 301–312.
[72] G. Qi, R.T. Yang, Appl. Catal. B 60 (2005) 13–22.
[73] T. Nanba, S. Masukawa, A. Ogata, J. Uchisawa, A. Obuchi, Appl. Catal. B 61 (2005) 288–296.
[74] G. Delahay, D. Valade, A. Guzmán-Vargas, B. Coq, Appl. Catal. B 55 (2005) 149–155.
[75] K.H. Rhee, F.R. Brown, D.H. Finseth, J.M. Stencel, Zeolites 3 (1983) 344–347.
[76] K.H. Rhee, V.U.S. Rao, J.M. Stencel, G.A. Melson, J.E. Crawford, Zeolites 3 (1983) 337–343.
[77] M.M. Mohamed, B.M. Abu-Zied, Thermochim. Acta 359 (2000) 109–117.
[78] B. Wichterlová, Y. Tvarůžková, Z. Sobalík, P. Sarv, Micropor. Mesopor. Mater. 24 (1998) 223–233.
[79] C. Pophal, T. Yogo, K. Yamada, K. Segawa, Appl. Catal. B 16 (1998) 177–186.
[80] Y. Li, J.N. Armor, Appl. Catal. B 1 (1992) L21–L29.
[81] F. Kapteijn, G. Marbán, J. Rodriguez-Mirasol, J. Molijn, J. Catal. 167 (1997) 256–265.
[82] R.S. da Cruz, A.J.S. Mascarenhas, H.M.C. Andrade, Appl. Catal. B 18 (1998) 223–231.
[83] J. Pérez-Ramírez, F. Kapteijn, A. Brückner, J. Catal. 218 (2003) 234–238.
[84] R.W. van den Brink, S. Booneveld, J.R. Pels, D.F. Bakker, M.J.F.M. Verhaak, Appl. Catal. B 32 (2001) 73–81.
[85] M. Kögel, V.H. Sandoval, W. Schwiege, A. Tissler, T. Turek, Chem. Ing. Tech. 70 (1998) 878–882.
[86] J. Pérez-Ramírez, F. Kapteijn, J.C. Groen, A. Doménech, G. Mul, J.A. Moulijn, J. Catal. 214 (2003) 33–45.
[87] C. Wagner, J. Chem. Phys. 18 (1950) 69–71.
[88] R.M. Dell, F.S. Stone, P.F. Tiley, Trans. Faraday Soc. 49 (1953) 201–209.
[89] J.-M. Herrmann, J. Disdier, Catal. Today 56 (2000) 389–401.
[90] T. Yamashita, A. Vannice, J. Catal. 161 (1996) 254–262.
[91] P. Pietrzyk, F. Zasada, W. Piskorz, A. Kotarba, Z. Sojka, Catal. Today 119 (2007) 219–227.
[92] E.J. Karlsen, M.A. Nygren, L.G.M. Pettersson, J. Phys. Chem. A 106 (2002) 7868–7875.
[93] G.S. Tschumper, H.F. Schaefer, J. Chem. Phys. 107 (1997) 2529–2541.
[94] A. Zecchina, L. Cerruti, E. Borello, J. Catal. 25 (1972) 55–64.
[95] V. Indovina, D. Cordischil, M. Occhiuzzi, A. Rieti, J. Chem. Soc. Faraday Trans. 1 75 (1979) 2177–2187.
[96] G.D. Pirngruber, P.K. Roy, Catal. Today 110 (2005) 199–210.
[97] D. Berthomieu, N. Jardillier, G. Delahay, B. Coq, A. Goursot, Catal. Today 110 (2005) 294–302.
[98] B. Wichterlová, J. Dědeček, A. Vondrová, J. Phys. Chem. 99 (1995) 1065–1067.
[99] Y.-F. Chang, J.G. McCarty, E.D. Wachsman, V.L. Wong, Appl. Catal. B 4 (1994) 283–299.
[100] T. Turek, J. Catal. 174 (1998) 98–108.
[101] V. Rakić, V. Rac, V. Dondur, A. Auroux, Catal. Today 110 (2005) 272–280.
[102] M.H. Groothaert, J.A. van Bokhoven, A.A. Battiston, B.M. Weckhuysen, R.A. Schoonheydt, J. Am. Chem. Soc. 125 (2003) 7629–7640.
[103] P.J. Smeets, M.H. Groothaert, R.A. Schoonheydt, Catal. Today 110 (2005) 303–309.
[104] M.H. Groothaert, P.J. Smeets, B.F. Sels, P.A. Jacobs, R.A. Schoonheydt, J. Am. Chem. Soc. 127 (2005) 1394–1395.
[105] L.J. Lobree, I.-C. Hwang, J.A. Reimer, A.T. Bell, J. Catal. 186 (1999) 242–253.
[106] M. Devadas, O. Kröcher, M. Elsener, A. Wokaun, G. Mitrikas, N. Söger, M. Pfeifer, Y. Demel, L. Mussmann, Catal. Today 119 (2007) 137–144.
[107] M. Iwamoto, H. Yahiro, Y. Mine, S. Kagawa, Chem. Lett. (1989) 213.
[108] Q. Zhu, R.M. van Teeffelen, R.A. van Santen, E.J.M. Hensen, J. Catal. 221 (2004) 575–583.
[109] G.I. Panov, V.I. Sobolev, A.S. Kharitonov, J. Mol. Catal. 61 (1990) 85–97.
[110] G.I. Panov, G.A. Sheveleva, A.S. Kharitonov, V.N. Romannikov, L.A. Vostrikova, Appl. Catal. A 82 (1992) 31–36.
[111] G.I. Panov, K.A. Dubkov, E.V. Starokon, Catal. Today 117 (2006) 148–155.
[112] K.A. Dubkov, N.S. Ovanesyan, A.A. Shteinman, E.V. Starokon, G.I. Panov, J. Catal. 207 (2002) 341–352.
[113] J. Dědeček, L. Čapek, B. Wichterlová, Appl. Catal. A 307 (2006) 156–164.
[114] J. Dědeček, B. Wichterlová, J. Phys. Chem. B 103 (1999) 1462–1476.
[115] C. Chupin, A.C. van Veen, M. Konduru, J. Després, C. Mirodatos, J. Catal. 241 (2006) 103–114.